IDENTIFYING VOLCANIC GLASS CONCENTRATION AND COMPOSITION WITH REMOTE SENSING USING MULTIVARIATE METHODS. C. J. Leight[1], M. C. McCanta[1], B. J. Thomson[1], and M. D. Dyar[2,3]. [1]Dept. of Earth & Planetary Sciences, Univ. of Tennessee, Knoxville TN 37996 (cleight@utk.edu), [2]Dept. of Astronomy, Mount Holyoke College, South Hadley, MA 01075, [3]Planetary Science Institute, Tucson, AZ 85719.

Introduction: Tephra are a common explosive volcanic product, typically composed of minerals, debris from previous eruptions, and glass (quenched melt) that provide information about the physical and chemical characteristics of the magma source region and eruptive vent [1–6]. Remote identification and non-destructive characterization of tephra are important for studies where sample collection may not be feasible, such as on other planetary bodies, where samples may be limited in size or where they are difficult to collect, such as in terrestrial deep-sea drill cores. Although the study of tephrochronology has not yet been applied to other bodies, potential extraterrestrial tephra deposits have been identified [e.g., 7–12] and the knowledge developed on terrestrial samples could be applied if identification methods are robust.

Previous studies have worked to identify tephra deposits using spectral features [e.g., 12, 13]. Band parameters in the 1 μm region have been used to successfully locate tephra layers in oceanic sedimentary settings [13]. However, extracting more information, such as glass composition or concentration, remains difficult using spectral band methods. Here we use multivariate partial least squares (PLS) analysis to both quantify and characterize the glass present in a tephra deposit using the entire spectral range.

Samples and Methods: This study utilizes 21 natural tephra samples from ten different terrestrial locations. Glass compositions range from 46–80 wt% SiO_2 and 5–15 wt% total alkali ($Na_2O + K_2O$), with a glass modal abundance of 40–91% (Table 1 of [14]). Bulk or whole rock compositions (glass + minerals and other eruptive debris) span the range 46–74 wt% SiO_2, and 4.2–12 wt% total alkali ($Na_2O + K_2O$).

Visible and near-infrared (VNIR: 0.35–2.5 μm) spectra were collected using an ASD Fieldspec4 at the University of Tennessee Knoxville (UTK). Bulk mid-infrared (MIR: 400–2500 cm^{-1}, or 4–25 μm) spectra were obtained with a Nicolet 6700 FTIR spectrometer at SUNY Stony Brook as described in [14]. Spectra of the >2 mm/>500 μm size fraction were not collected for the MIR [14]. Major and minor element analyses were completed on the Cameca SX-100 electron microprobe at UTK. Phase abundances were measured using the Phenom Pro XL scanning electron microscope at UTK following the methods of [13,15].

VNIR and MIR spectra and compositional data were analyzed using the Data Exploration and Visualization Analysis of Spectra (DEVAS) website ([16]; http://nemo.mtholyoke.edu/). Partial least squares (PLS) regressions were used to model the relationship between VNIR and MIR spectra of the natural tephra samples and various compositional parameters. Separate PLS models were built for both the VNIR and MIR spectra to predict the modal abundance of glass present in each sample, as well as the SiO_2 wt% of both the glass and bulk sample, and size fraction.

The spectra were baseline corrected (continuum removed) and normalized using several methods (**Table 1**) to optimize the root mean square error with K-fold cross-validation (RMSE-CV) of each regression model, using nine folds. The combination of baseline removal and normalization routine for each PLS model was chosen to yield the lowest RMSE-CV for each predictive model, and therefore each PLS model calls for a unique combination (**Table 1**). The inclusion of this step greatly increases the accuracy of the PLS models by removing run-to-run variations in spectra.

Results: All PLS models required some amount of preprocessing in the form of baseline removal or normalization, frequently both. The preprocessing steps and predictions for each PLS model are given in **Table 1**. **Fig. 1** gives predictions for each model. Uncertainty (calculated as RMSE-CV) of each model is reported in **Table 1**, and the goodness-of-fit of the models are reported as the R^2. The MIR PLS models have

Table 1. VNIR and MIR PLS model parameters

	Predicted Variable	Normalization	Baseline Correction	Components	R^2	RMSE-CV
VNIR	Glass Phase %	Max	Kaijfosz-Kwiatek [21]	2	0.60	±0.12 %
	Glass wt % SiO_2	L2	ASL [21]	5	0.85	±6.05 wt%
	Bulk wt % SiO_2	Max	ASL [21]	9	0.96	±4.30 wt%
	Grain Size	Min	-	2	0.08	±393 μm
MIR	Glass Phase %	Cumulative	Tophat [22]	4	0.77	±0.12 %
	Glass wt % SiO_2	Cumulative	MedianFilter [21]	9	0.94	±4.02 wt%
	Bulk wt % SiO_2	Cumulative	ASL [21]	5	0.98	±3.39 wt%
	Grain Size	Cumulative	MPLS [21]	7	0.89	±339 μm

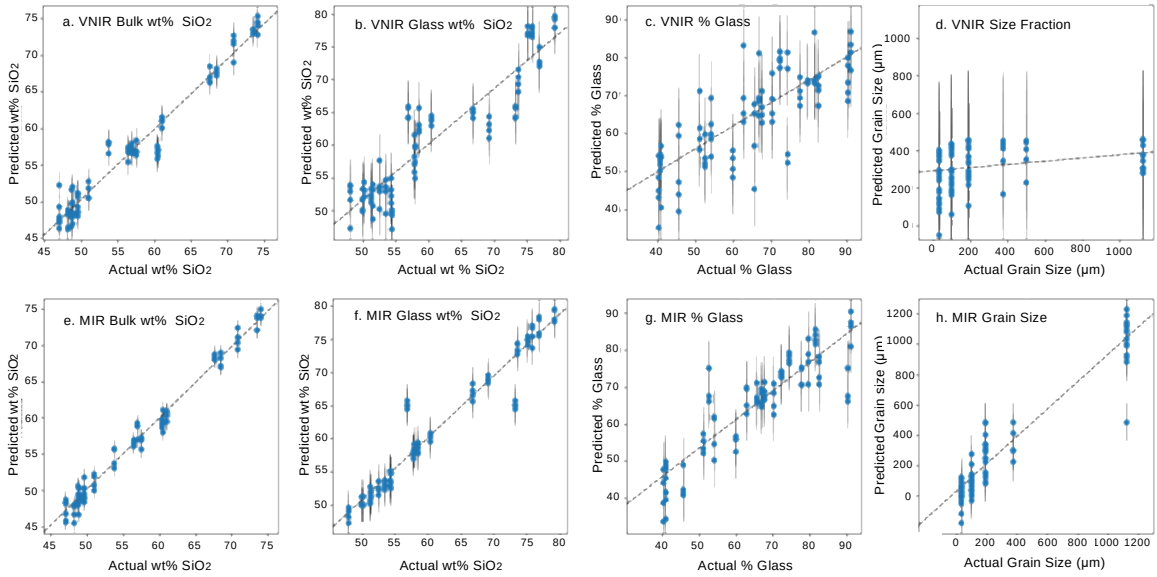

Figure 1. Results of predictions by PLS models for both the VNIR and MIR. Size fraction predictions are as follows: <63 µm, 63–125 µm, 125–250 µm, 250–500 µm or 250 µm–2 mm, and >500 µm or >2 mm. Prediction error is shown by the vertical black error bars. Measurement error (*x*-axis) is within the size of the points. Dashed line shows line of best fit.

consistently better R^2 and accuracies than the VNIR models when predicting variables.

VNIR Modeling Results: Using VNIR data, PLS models for bulk SiO_2 (**Fig. 1a**) are accurate to ±4.30 wt%, while the SiO_2 content of glass can be predicted to ±6.05 wt% (**Fig. 1b**). The amount of glass can be predicted to ±0.12 modal % (**Fig. 1c**). PLS models using VNIR spectra do a poor job of predicting grain size (**Table 1, Fig. 1d**), with an R^2 of 0.08.

MIR Modeling Results: PLS models built using MIR spectra are consistently equal to or better than those based on the VNIR data: ±3.39 wt% for bulk SiO_2 (**Fig. 1e**), ±4.02 wt% SiO_2 in the glass (**Fig. 1f**), ±0.12 modal % (**Fig. 1g**) for the amount of glass present, and ±0.34 µm (**Fig. 1h**) for grain size.

Discussion: This work demonstrates that PLS models can accurately quantify glass abundance and compositional information using either VNIR and MIR spectra in volcanic tephra. The multivariate models have better accuracy than other studies have achieved using spectral band parameters [e.g., 12, 13]. Moreover, both the bulk and glass wt % SiO_2 composition can be measured with these methods in a non-destructive and non-disruptive manner. Calculated RMSE accuracies (**Table 1**) for both the VNIR and MIR PLS models suggest their predictive capabilities vary, indicating that while both spectral regions can be used for characterization of glass-bearing deposits, the MIR is nominally better for predictions.

The PLS analysis, which works using linear combinations for the regressions [17], produces more accurate results from the MIR spectra, likely because the MIR region more readily deconvolves in a linear manner [18] than the VNIR. Spectra in the VNIR region do not add linearly [e.g., 19, 20], and thus bands cannot be directly attributed to a compositional parameter such as bulk wt% SiO_2, particularly because the spectra utilized here do not represent a single phase, or even a three-phase mixture.

This work highlights the importance of the MIR PLS models, suggesting that developing a better understanding of glassy tephra deposits remotely requires increased emphasis on high-spectral-resolution MIR instruments. However, the more-commonly available VNIR spectra still remain useful in performing bulk characterization and establishing the presence and abundance of glass.

References: [1] Anderson A.T. et al. (2000) *J. Petrology, 41*(3), 449-473. [2] Saal A.E. et al. (2008) *Nature, 454*, 192-195. [3] Hauri E.H. et al. (2018) *Geology, 46*(1), 55-58. [4] Lowe D.J. (2011) *Quat. Geochron., 6*(2), 107-153. [5] Payne R. et al. (2008) *Quat. Research, 69*(1), 42-55. [6] Shane P. (2000) *Earth-Sci. Rev. 49*(1-4), 223-259. [7] Wilson L. and Head J. (1994) *Rev. Geophys. 32*(3), 221-263. [8] Papike J.J. et al. (1982) *Rev. Geophys, 20*(4), 761-826. [9] Delano J.W. (1986) *JGR, 91*(B4), 201-213. [10] Horgan B. and Bell J.F. (2012) *Geology 40*(5), 391-394. [11] Kerber L. et al. (2011), *PSS, 59*, 1895. [12] Horgan B. et al. (2014) *Icarus, 234*, 132-154. [13] McCanta M.C. et al., (2015) *G-cubed, 16, 4029.* [14] Leight C. et al. (2019) *LPSC 50*, abstract #2747. [15] Cassidy M. et al. (2014) *Earth-Sci. Rev. 138*, 137-155. [16] Carey C. et al. (2017) *LPSC 48*, abstract #1097. [17] Hastie T. et al., (2017) *Springer Sci. & Business Media* 80-81. [18] Ramsey M.S. and Christensen P.R. (1998) *JGR, 103*, 577. [19] Adams J.B. and Filice A.L. (1967) *JGR, 72*(22), 5705-5715. [20] Crown D.A. and Pieters C.M. (1987) *Icarus*, 492-506. [21] Dyar et al. (2016) *Spectroch. Acta B, 126*, 53-6.4 [22] Perez-Pueyo et al. (2010) *App. Spec., 64*(6) 595-600.